FEEDBACK CONTROL SYSTEMS FOR NON-LINEAR SIMULATION OF OPERATIONAL TRANSIENTS IN LMFBRs

M. Khatib-Rahbar, A. K. Agrawal and E. S. Srinivasan

Department of Nuclear Energy
Brookhaven National Laboratory
Upton, New York 11973 USA

MASTER

NOTICE
This report was prepared as an account of work sponsored by the United States Government. Neither the United States nor the United States Department of Energy, nor any of their employees, nor any of their contractors, subcontractors, or their employees, makes any warranty, express or implied, or assumes any legal liability or responsibility for the accuracy, completeness or usefulness of any information, apparatus, product or process disclosed, or represents that its use would not infringe privately owned rights.

ABSTRACT

Feedback control systems for non-linear simulation of operational transients in LMFBRs are developed. The models include (1) the reactor power control and rod drive mechanism, (2) sodium flow control and pump drive system, (3) steam generator flow control and valve actuator dynamics, and (4) the supervisory control. These models have been incorporated into the SSC code using a flexible approach, in order to accommodate some design dependent variations. The impact of system nonlinearity on the control dynamics is shown to be significant for severe perturbations. Representative result for a 10 cent and 25 cent step insertion of reactivity and a 10% ramp change in load in 40 seconds demonstrate the suitability of this model for study of operational transients without scram in LMFBRs.

INTRODUCTION

Adequate modeling of Plant Control Systems (PCS) for the study of Anticipated Transients Without Scram (ATWS) is of considerable significance in the design, operation and safety evaluation of Liquid-Metal-Cooled Fast Breeder Reactor (LMFBR) systems. In order to assess the system response to such high frequency, low consequence transients, detailed models for plant control systems must, therefore, be provided in any large simulation code.

Limited modeling of PCS have been developed and included in a number of system simulation codes[1,2,3] which do not adequately represent the actual controls that are present in an LMFBR plant.

The aim of this paper is to present a fairly generalized feedback control model that has been developed for the Super System Code (SSC).[4] This model has been formulated to be more easily adaptable to plants of similar design and control characteristics, using the digital computer mechanizations

DISTRIBUTION OF THIS DOCUMENT IS UNLIMITED

DISCLAIMER

This report was prepared as an account of work sponsored by an agency of the United States Government. Neither the United States Government nor any agency Thereof, nor any of their employees, makes any warranty, express or implied, or assumes any legal liability or responsibility for the accuracy, completeness, or usefulness of any information, apparatus, product, or process disclosed, or represents that its use would not infringe privately owned rights. Reference herein to any specific commercial product, process, or service by trade name, trademark, manufacturer, or otherwise does not necessarily constitute or imply its endorsement, recommendation, or favoring by the United States Government or any agency thereof. The views and opinions of authors expressed herein do not necessarily state or reflect those of the United States Government or any agency thereof.

DISCLAIMER

Portions of this document may be illegible in electronic image products. Images are produced from the best available original document.

of feedback control equations in the time domain. The detailed plant model with its associated nonlinearities is coupled to the controllers through various feedback cascades for (1) reactor power control, (2) primary and intermediate system sodium flow-speed control, (3) steam generator flow control, and (4) the plant supervisory control.

The controller electronics is represented by proportional-integral-derivative (PID) actions. The model includes the dynamics of process measurement sensors and transmitters, and also provides for the presence of deadbands and saturation on the controller outputs during manual and automatic modes of operation. The reactor control rod drive mechanism is represented by a multi-bank rod system within the framework of the first order perturbation theory. The sodium pump-drive model allows for both rheostatic (wound-rotor) as well as variable frequency (squirrel cage) type speed controllers. The model for valve dynamics simulated the valve drive mechanism including deadband and hysterics effects.

The impact of system nonlinearity on the control dynamics is demonstrated by comparing the present nonlinear model with a linear counterpart for the intermediate loop flow-speed controller.

Representative results for 10 cent and 25 cent step insertions of reactivity and a typical plant unloading are also presented.

UNIT CONTROLLER

The purpose of the plant control systems is to maintain the plant at the desired power, temperature, pressure and flow rates during startup, load changing, power operation and shutdown conditions.

Several modes of control action can be used to process the deviation from the setpoint of the controlled variable, namely: proportional, integral, and derivative action. They may be used separately or in combinations depending upon the situation,[5,6] using the feedforward with feedback approach.

A block diagram representation of a unit controller is shown in Figure 1. It is seen that the unit controller is composed of the setpoint generator, process measuring device, deadband and a proportional-integral-derivative (PID) module.

The setpoint generator allows for the generation of process setpoint either through the supervisory controller, X_D or a manual switch X_{SP} of Figure 1. Plant control systems include measuring instrument sensors and transmitters which monitor the process variables important for the operation of the controller. To account for instrumentation time lags, the response of these sensors and transmitters are modeled by the following first order equation:

$$\tau_M \frac{dX_M}{dt} = X - X_M \qquad (1)$$

The deviation signal can then be calculated as:

$$\varepsilon = \begin{cases} X_D - X_M & \text{Automatic} \\ X_{SP} - X_M & \text{Manual} \end{cases} \tag{2}$$

There is normally a deadband around the setpoint, of width $2\varepsilon_0$, over which the controller is insensitive to the changes in the error (deviation) signal, i.e., $\varepsilon = 0$, if $|\varepsilon| \leq \varepsilon_0$.

This error signal is then fed to a PID module to generate a trim signal as follows:

$$Tr = K\left(\varepsilon + R\int \varepsilon\, dt + \tau_D \frac{d\varepsilon}{dt}\right) \tag{3}$$

where K is the proportional gain, R is the integral reset rate (s^{-1}) and τ_D is the derivative time(s). In order to prevent undesirable oscillations and cyclic disturbances under certain control conditions, the controllers are usually designed to limit the excessive integral roll-up and roll-down.[7] This effect has been accounted for by bounding the value of the integral in Equation (3). The trim signal, Tr, is the controller output signal which is used as an input to the next unit controller or as an input to the actuator.

In the SSC code, as many as five unit (cascade) controllers can be placed in series to represent multiple feedback loops which may exist in various plant controllers as will be discussed in the following subsections.

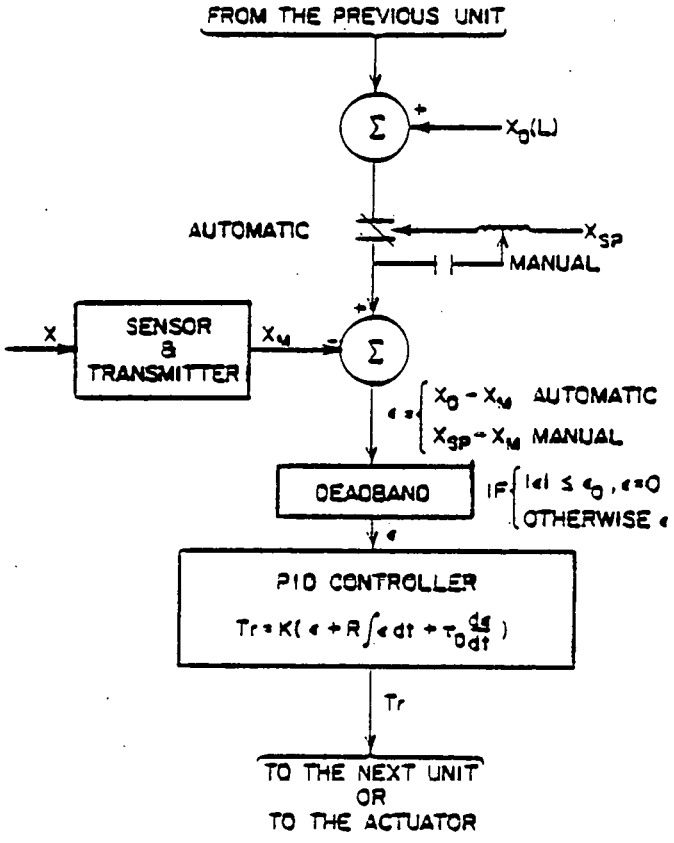

Figure 1. Block Diagram of the Unit Controller.

Supervisory Control

The supervisory control system uses the demanded power (load) signal and transforms it into a feedforward demand for the various controllers in order to maintain the desired operating conditions. A typical part load profile of some key plant variables is shown in Figure 2. This part load profile is generated by performing steady-state calculations at various power levels assuming constant turbine throttle conditions. The load-dependent setpoints can therefore be calculated using polynomial approximations of the form:

$$X_D = \sum_{i=0}^{2} c_i L^i \quad . \tag{4}$$

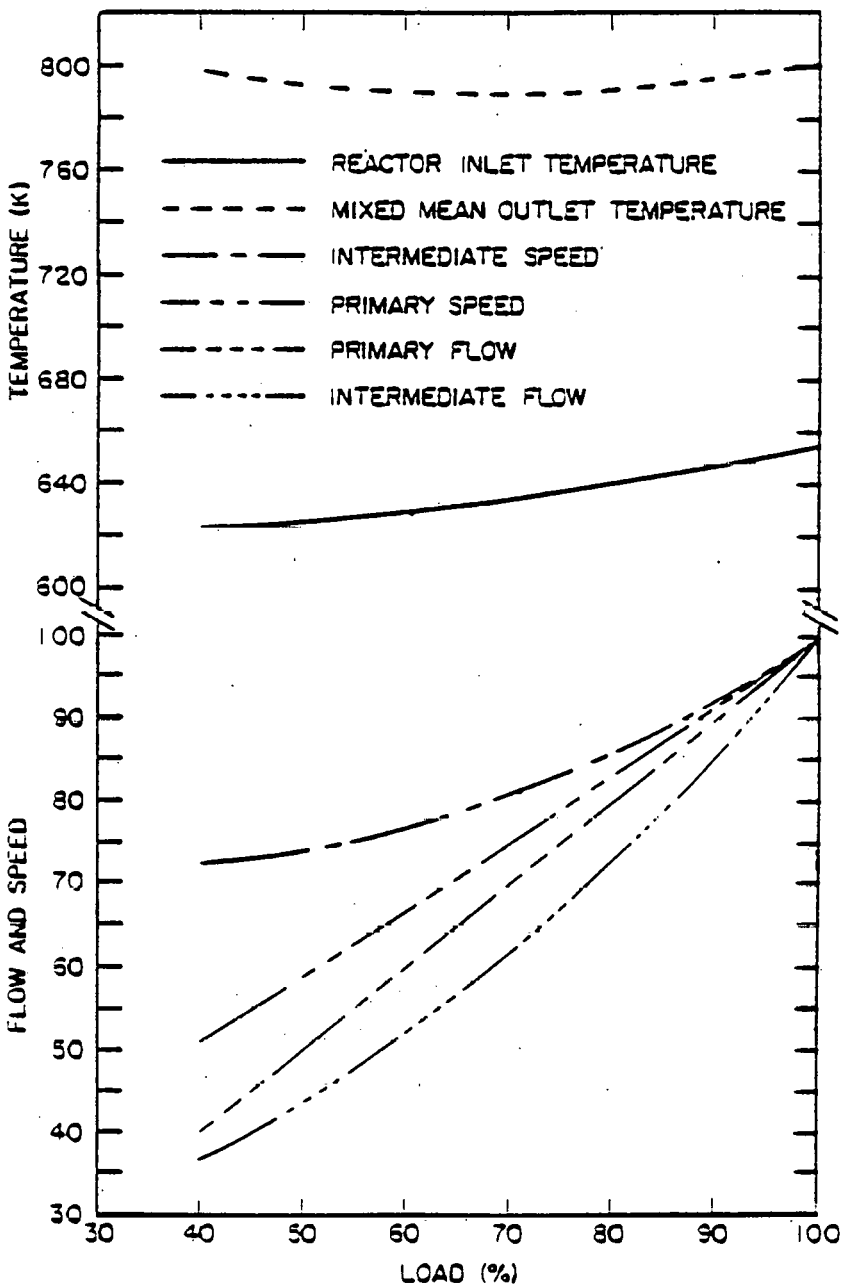

Figure 2. Part Load Profile

Reactor Power Control

The primary control rods are used for both power regulation and reactor shutdown, while the secondary control rods are used for shutdown only. The present model represents the primary control rods by several banks which are assumed to be ganged according to a specified scheme and the reactivity worth of each rod bank is given by first order perturbation theory[8] as:

$$\rho_{PR} = \sum_{i=1}^{M} \rho_{max,i} \left[(Z_i/Z_{max,i}) - \frac{1}{2\pi} \text{Sin } (2\pi Z_i/Z_{max,i}) \right] \tag{5}$$

The control rod position is regulated by the reactor power controller and rod drive mechanism. The reactor control system positions the control rods to reach the desired reactor thermal power, sodium and steam temperatures according to the part load profile. The output of the controller is sent to the power dead zone and saturation circuit limits of the control rod rates. Finally, the signal is divided into an analog magnitude signal and a digital direction signal for use as demands to the control rod drive mechanism actuator.

The input circuitry to each controller accepts on-off inputs for IN, OUT and HOLD commands and provides the required action. The IN command steps a single rod down in the core at a predetermined rate. The OUT command steps a single rod up out of the core at a predetermined rate (not necessarily the same as the IN rate) and the HOLD command maintains the rod in its present position (no motion); that is:

$$\frac{dZ_i}{dt} = \begin{cases} V_{down} & \text{IN Command} \\ V_{up} & \text{OUT Command} \\ 0 & \text{HOLD Command} \end{cases} \tag{6}$$

Sodium Flow Control

The dynamics of sodium flow inside the primary and intermediate systems are governed by the momentum equation which can be written as[4,9]:

$$\left(\frac{\ell}{A}\right) \frac{dW}{dt} + (P_{in} - P_{out}) + \delta P_g + \delta P_f + \delta P_m + \delta P_p = 0 \tag{7}$$

The pump pressure rise, δP_p is dependent on pump speed and sodium flow rate, as described by Madni, et al.[9]

The dynamics of the pump is governed by the torque balance equation for the shaft and rotating assembly[3,4,9] as:

$$\left(\frac{2\pi}{60}\right)\left(\frac{I\Omega_D}{\Gamma_D}\right) \frac{d\alpha}{dt} = \beta_{Mt} - \beta_{F\ell} - \beta_{Fr} \tag{8}$$

The hydraulic torque, $\beta_{F\ell}$, and the friction torque, β_{Fr} are complicated functions of pump operating conditions and can be found elsewhere.[3,9]

During normal operation, the drive motor torque is adjusted by the controller action, in order to maintain the desired operating conditions. For example, a slight decrease in load causes a reduction in the motor torque which in turn leads to a decrease in pump speed and eventually the sodium flow rate through the variation in pump head, δP_p.

There are various methods for achieving speed control through adjustment of the drive motor torque.[10] They include: (1) changing the number of poles, (2) changing the frequency, (3) changing the external resistance, and (4) varying the hydraulic coupling. The method applied depends on the motor type, and the adequacy of control over the desired operating regime. In the present analysis, we will discuss the frequency and the rheostatic methods for speed control.

The torque of the squirrel cage motor can be written as[10]:

$$\beta_{Mt} = (a_1 \, s + \frac{b_1}{s})^{-1} \tag{9}$$

where a_1, b_1 are constants characterizing the motor behavior and s is the slip ratio defined by $1 - (\Omega_D/\Omega_S)\alpha$, Ω_S being the synchroneous speed (rpm) which is related to frequency f(Hz) and the number of pairs of poles p by (60 f/p).

The torque of the wound rotor induction motor can also be represented by a similar relationship[10]:

$$\beta_{Mt} = (a_2 \frac{s}{R} + b_2 \frac{R}{s})^{-1} \tag{10}$$

and,

$$R = 1 + \frac{R_{ext}}{R_M} \tag{11}$$

where a_2, b_2 are constants characterizing the motor behavior, R is the external resistance parameter, and R_{ext} is the variable external resistance provided by a liquid rheostat actuator and added in series to R_M, the motor rotor resistance (Ω) which is related to the liquid rheostat electrode position y according to the following equation:

$$R_{ext} = R_{max} \, (1 - y)^3 \tag{12}$$

The variable frequency or the liquid rheostat electrode position can be simulated using a second order equation representing a mechanical actuator behaving as a damped harmonic oscillator[6]:

$$\frac{1}{\omega_n^2} \frac{d^2h}{dt^2} + \frac{2\zeta}{\omega_n} \frac{2h}{dt} + (h - h_i) = Tr \tag{13}$$

where ω_n is the natural frequency; ζ is the damping coefficient, h is the actuator output (frequency or the electrode position), h_i is the initial output, and Tr is the trim signal from the last unit controller.

Steam Generator Control

The purpose of steam generator control system is to maintain the temperature, pressure and flow rates at the desired level for both normal and off normal operating conditions. The steam generator control systems consist of (a) feedwater system, and (b) turbine and dump flow mechanism.

The recirculation type steam generator consists of a steam drum, evaporators and superheaters, and a steam header. The feedwater flow rate is controlled in order to maintain a desired steam drum water level and minimize the difference between the feedwater flow into the drum and the saturated steam flow out of the drum. The steam flow rate out of the steam header is controlled based on near constant pressure at the turbine. To enable the nuclear steam supply system to follow turbine load reductions which may exceed large step or ramp changes, an artificial steam load is incorporated. This load is created by dumping steam from the steam header to either condenser and/or atmosphere. The dump system is controlled to give the required ramp load changes to prevent reactor scram. Following the trip, the dump system is switched to a closed loop pressure control mode based on constant header pressure.

The steam generator unit controller is identical to that described earlier. Here, the controller output is used either to adjust the feedwater pump speed and/or to change a valve stem position.

The valve dynamics is represented by a first order system accounting for deadband and hysterisis effects. That is:

$$\frac{dS_v}{dt} = \begin{cases} \dfrac{1}{\tau_{vo}} & Tr \geq Tr_{max} \quad \text{(opening)} \\ 0 & Tr_{min} < Tr < Tr_{max} \quad \text{(no motion)} \\ \dfrac{1}{\tau_{vc}} & Tr \leq Tr_{min} \quad \text{(closing)} \end{cases} \tag{14}$$

and the fractional stem position S_v is bounded; i.e., $S_{min} \leq S_v \leq S_{max}$. Here, S_{min} is the minimum stem position, S_{max} is the maximum stem position, τ_{vo} is the time to open from S_{min} to S_{max}, and τ_{vc} is the time to close from S_{max} to S_{min}. The deadband and hysterisis effects prevent the valve from opening if the trim signal is smaller than a maximum limit, Tr_{max}, and from closing if the trim is greater than a minimum limit Tr_{min}.

Non-Linearity Effects

The control systems discussed in this paper have been incorporated into the SSC code. SSC models and numerically solves the conservation equations described in the previous subsections, in their truly nonlinear forms.

Many of the existing control system design and analysis studies use linearized approximations representative of the nonlinear systems in the vicinity of the steady-state operating conditions. While much useful information can be obtained from such studies, it frequently is desirable or necessary to consider nonlinearities in control system design and operation.

In order to demonstrate the comparison between the linear and nonlinear models, a linearized version of the flow-speed control was developed by using Taylor series expansions of the nonlinear terms in the coolant momentum and the pump angular momentum equations around the steady-state 100% operating conditions. The two models were compared for a transient resulting from a 20% step reduction in load demand. Figure 3 shows the system response for both linear and nonlinear models using identical controller settings (gains, time constants, etc.).

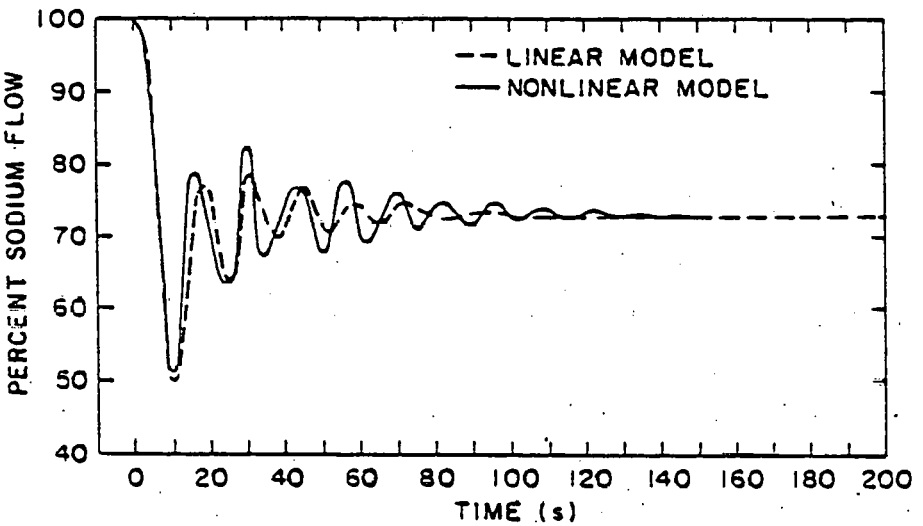

Figure 3. Comparison of Linear and Non-Linear Models.

It is evident that the flow oscillations are less severe and tend to damp-out much sooner for the linear model than for the nonlinear model. Several perturbations were tested and it was found that the agreement between the linear and nonlinear models improve as the input perturbations get less severe. It was also observed that for a just stable control system setting with the linearized model, the nonlinear model was unstable.

RESULTS AND DISCUSSIONS

The present model has been tested using the Clinch River Breeder Reactor Plant (CRBRP) reference design data where available.[11]

Table I summarizes various feedback elements and their associated control settings for reactor power, primary and intermediate flow-speed control systems. Table II sets forth the primary control rod banking data.

TABLE I
Plant Control System Data

Unit Controller			τ_m(s)	K	R(s^{-1})	τ_D(s)	ϵ_o	Actuator Constants
Reactor Power Controller		Steam Temperature	0.20	2.0	0	0	0	$v_{up} = 3.81 \times 10^{-3}$ m/s $v_{down} = -3.81 \times 10^{-3}$ m/s
		Core Mixed Mean Temp.	0.20	2.0	0	0	0	
		Neutron Flux	0.05	1.0	0	0	0.005	
Flow Controller	Primary	Reactor Inlet Temp.	0.20	1.0	0	0	0	$a_1 = 0.577$ $b_1 = 0.065$ $\zeta = 1.0$ (critically damped) $\omega_n = 0.375$ (s^{-1}) $\Omega_D = 1116$ rpm
		Sodium Flow	0.50	1.0	0	0	0	
		Pump Speed	0.02	1.0	0.10	0	0.005	
	Intermediate	Steam Pressure	0.15	1.0	0.02	0	0	$a_1 = 0.577$ $b_1 = 0.065$ $\zeta = 1.0$ $\omega_n = 0.375$ $\Omega_D = 1116$ rpm
		Sodium Flow	0.50	1.0	0.20	0	0	
		Pump Speed	0.02	1.0	0.10	0	0.005	

TABLE II
Primary Control Rod Banking Data[11]

Location	$\rho_{max,i}$($)	$Z_{max,i}$(m)	ρ_i($)	Z_i(m)
6-R7F	12.17	0.940	3.49	0.300
6-R7C	11.00	0.940	6.72	0.584
2-R4	2.95	0.940	2.95	0.940

Three representative anticipated transients without scram were simulated, they are: (1) a 10 cent step insertion of reactivity, (2) a 25 cent step insertion of reactivity and (3) a 10% ramp change in load demand in 40 seconds.

Figure 4 shows the reactor system response to a 10 cent and a 25 cent step insertions of reactivity at time zero of the transient. The total reactivity is seen to jump from 0 to 0.10 and 0.25 dollar at time zero causing a sharp rise in the neutron flux (power level) and, hence, an increase in reactor temperatures. The controller tries to correct for the disturbance by driving the regulatory bank into the core, until finally the neutron flux and the core mixed mean sodium temperature reach their respective setpoints as calculated by the plant supervisory controllers.

It is important to note that all of the automatic shutdown functions of the Plant Protection System (PPS), which would normally override the controllers in an event that the PPS settings are exceeded (e.g., 115% overpower signal) were inactivated.

Figure 5 illustrates the plant response to a typical plant unloading of 10% in 40 seconds. It is seen that as the load demand is reduced, the plant control system responds by driving the regulating rod into the reactor as well as reducing the drive motor torque on both primary and intermediate pumps causing the desired reduction in the feedback variables to within the accuracies of their deadband settings.

From the results presented, the following conclusions are derived: (1) the representation of plant control systems in a large system simulation code is an essential tool for the study of ATWS event in LMFBR systems, and (2) the nonlinearity of the plant over a wide range of operating conditions necessitates a nonlinear simulation of the overall system.

For future work, it is essential to include improved models to simulate the motor-generator set and its influence on the sodium flow-speed control system. The influence of unit controller settings and feedback cascading on the predicted response of the plant requires further investigation. The interaction of the plant protection and control systems needs to be studied to determine the possibility of PCS adversely affecting or preventing the PPS actions.

ACKNOWLEDGEMENT

The authors acknowledge the invaluable help of J. G. Guppy and R. J. Kennett in interfacing the present model into the SSC code. Thanks are also due to I. K. Madni for reviewing the paper, and to Ms. D. Clay for her skillful typing of this manuscript.

This work was performed under the auspices of the United States Nuclear Regulatory Commission.

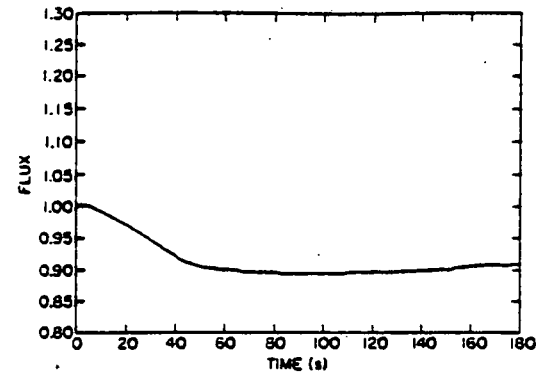

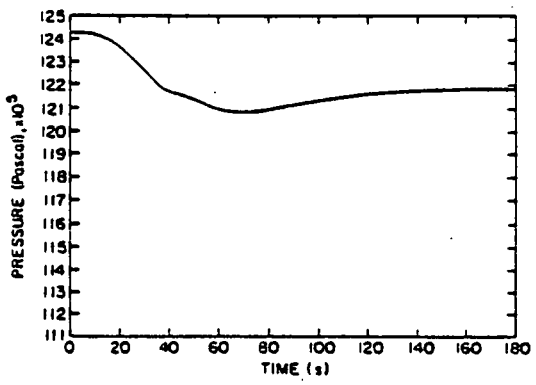

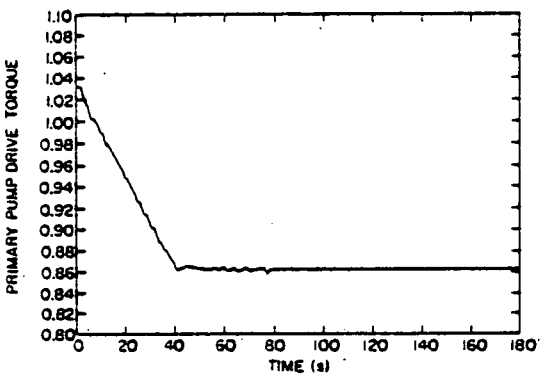

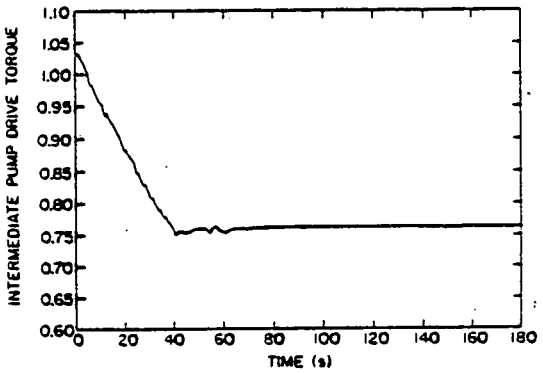

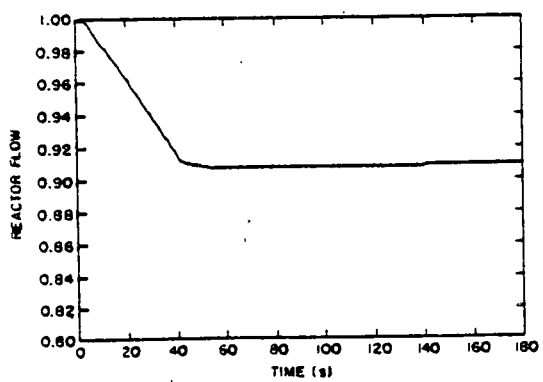

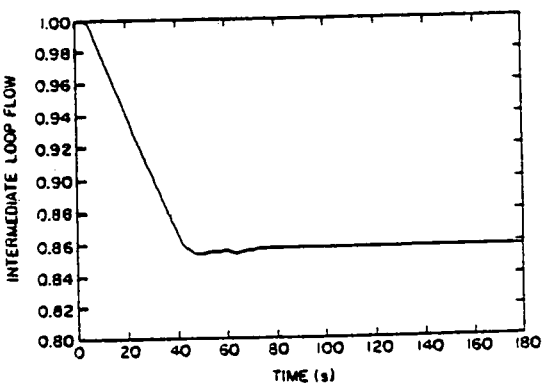

Figure 5. System Response to a Transient Resulting from a 10% Ramp Change in Power Demand in 40 Seconds.

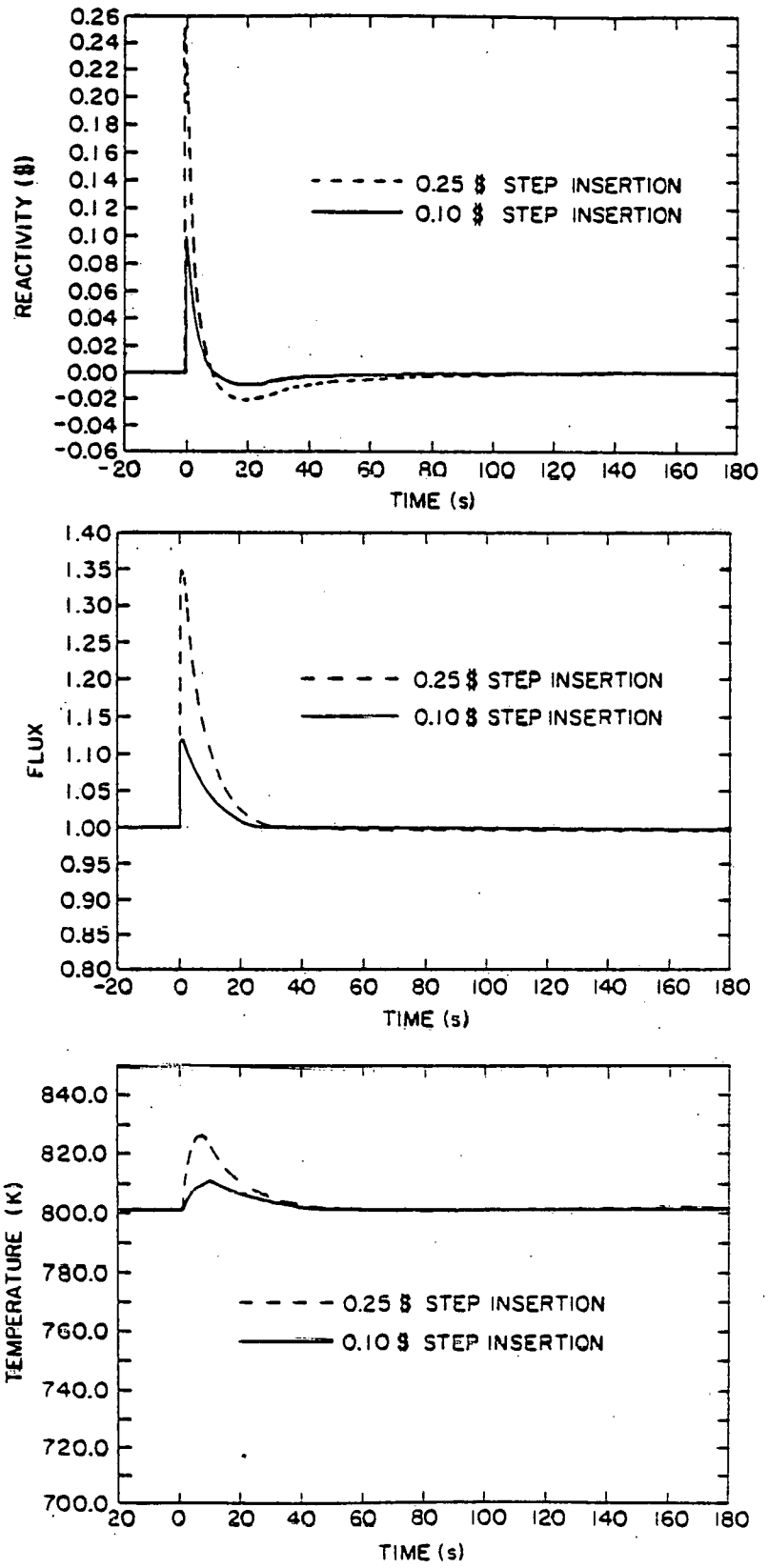

Figure 4. System Response to 10 cent and 25 cent Step Insertion of Reactivity Transient.

NOMENCLATURE

A	Area (m^2)
a	Motor constant
b	Motor constant
c	Polynomial coefficient
f	Frequency (Hz)
h	Actuator output
I	Inertia ($kg-m^2$)
K	Gain
L	Load
ℓ	Length (m)
P	Pressure (N/m^2)
p	Pairs of poles
R	Repeat rate, resistance (s^{-1}, Ω)
S	Stem position
s	Slip
Tr	Trim
V	Control rod speed (m/s)
W	Flow rate (kg/s)
X	Process variable
y	Electrode position
Z	Rod position (m)
α	Relative speed
β	Relative torque
ε	Error
ζ	Damping coefficient
τ	Time constant (s)
Ω	Speed (rpm)
ω	Natural frequency (s^{-1})
Γ	Torque (N-m)

Subscripts:

D	Demand/derivative/design
ext	External
f	Friction
Fl	Fluid
Fr	Friction
g	Gravity
M	Measured, momentum
Mt	Motor
s	Synchronous
SP	Set point

REFERENCES

1. "LMFBR Demonstration Simulation Model, DEMO," Westinghouse Advanced Reactors Division, WARD-D-0005 (Rev. 4), (1976).

2. D. L. HETRICK and G. W. SOWERS, "BRENDA: A Dynamic Simulator for a Sodium-Cooled Fast Reactor Power Plant," U. S. Nuclear Regulatory Commission, NUREG/CR-0244 (1978).

3. K. B. CADY et al., "EPRI-CURL: Dynamic Analysis of Loop-Type LMFBRs," Electric Power Research Institute, EPRI-NP-1001 (1979).

4. A. K. AGRAWAL et al., "An Advanced Thermohydraulic Simulation Code for Transients in LMFBRs (SSC-L)," Brookhaven National Laboratory, BNL-NUREG-50773 (1978).

5. D. M. CONSIDINE, (editor), *Process Instruments and Controls Handbook*, Gordon and Breach, Science Publishers, Inc., New York (1969).

6. D. R. COUGHANOWR and L. B. KOPPEL, *Process Systems Analysis and Control*, McGraw-Hill Book Co., New York (1965).

7. "Operator's Manual for Vutronik Cascade Control Stations," Operator's Manual 37-01-05, Issue 2, Honeywell Industrial Division, Fort Washington, Pennsylvania (1973).

8. J. R. LAMARSH, *Introduction to Nuclear Reactor Theory*, Addison-Wesley Publishing Company, Inc., Massachusetts (1961).

9. I. K. MADNI, E. G. CAZZOLI, and A. K. AGRAWAL, "A Single-Phase Sodium Pump Model for LMFBR Thermal-Hydraulic Analysis," in *Proc. of International Meeting on Fast Reactor Safety Technology*, August 19-23, 1979, Seattle, Washington.

10. P. L. ALGER, *Induction Machines*, Gordon and Breach Science Publishers, New York (1970).

11. Clinch River Breeder Reactor Plant Preliminary Safety Analysis Report, Project Management Corporation (1975).

The deviation signal can then be calculated as:

$$\varepsilon = \begin{cases} X_D - X_M & \text{Automatic} \\ X_{SP} - X_M & \text{Manual} \end{cases} \tag{2}$$

There is normally a deadband around the setpoint, of width $2\varepsilon_0$, over which the controller is insensitive to the changes in the error (deviation) signal, i.e., $\varepsilon = 0$, if $|\varepsilon| \leq \varepsilon_0$.

This error signal is then fed to a PID module to generate a trim signal as follows:

$$Tr = K\left(\varepsilon + R\int \varepsilon\, dt + \tau_D \frac{d\varepsilon}{dt}\right) \tag{3}$$

where K is the proportional gain, R is the integral reset rate (s^{-1}) and τ_D is the derivative time(s). In order to prevent undesirable oscillations and cyclic disturbances under certain control conditions, the controllers are usually designed to limit the excessive integral roll-up and roll-down.[7] This effect has been accounted for by bounding the value of the integral in Equation (3). The trim signal, Tr, is the controller output signal which is used as an input to the next unit controller or as an input to the actuator.

In the SSC code, as many as five unit (cascade) controllers can be placed in series to represent multiple feedback loops which may exist in various plant controllers as will be discussed in the following subsections.

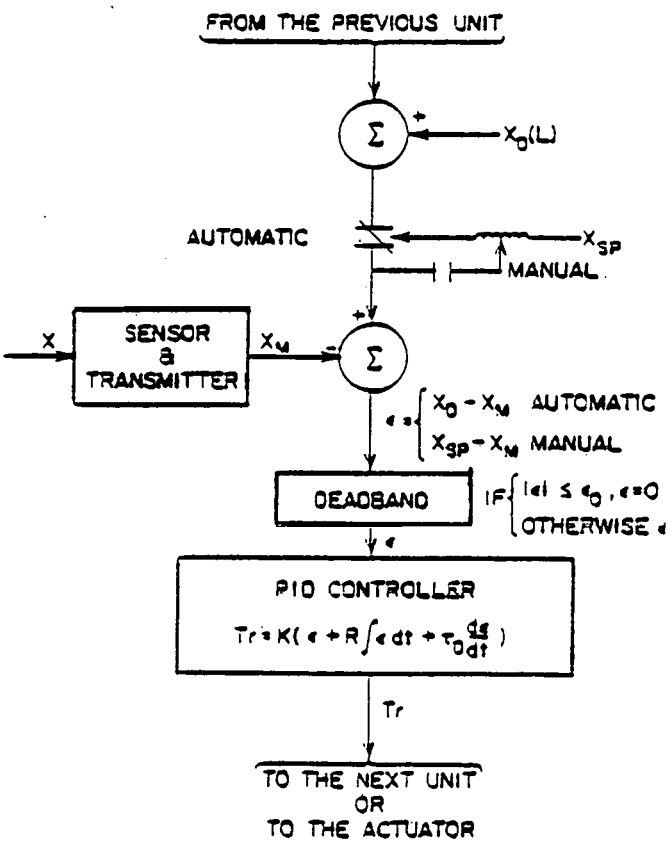

Figure 1. Block Diagram of the Unit Controller.

Supervisory Control

The supervisory control system uses the demanded power (load) signal and transforms it into a feedforward demand for the various controllers in order to maintain the desired operating conditions. A typical part load profile of some key plant variables is shown in Figure 2. This part load profile is generated by performing steady-state calculations at various power levels assuming constant turbine throttle conditions. The load-dependent setpoints can therefore be calculated using polynomial approximations of the form:

$$X_D = \sum_{i=0}^{2} c_i L^i \quad . \tag{4}$$

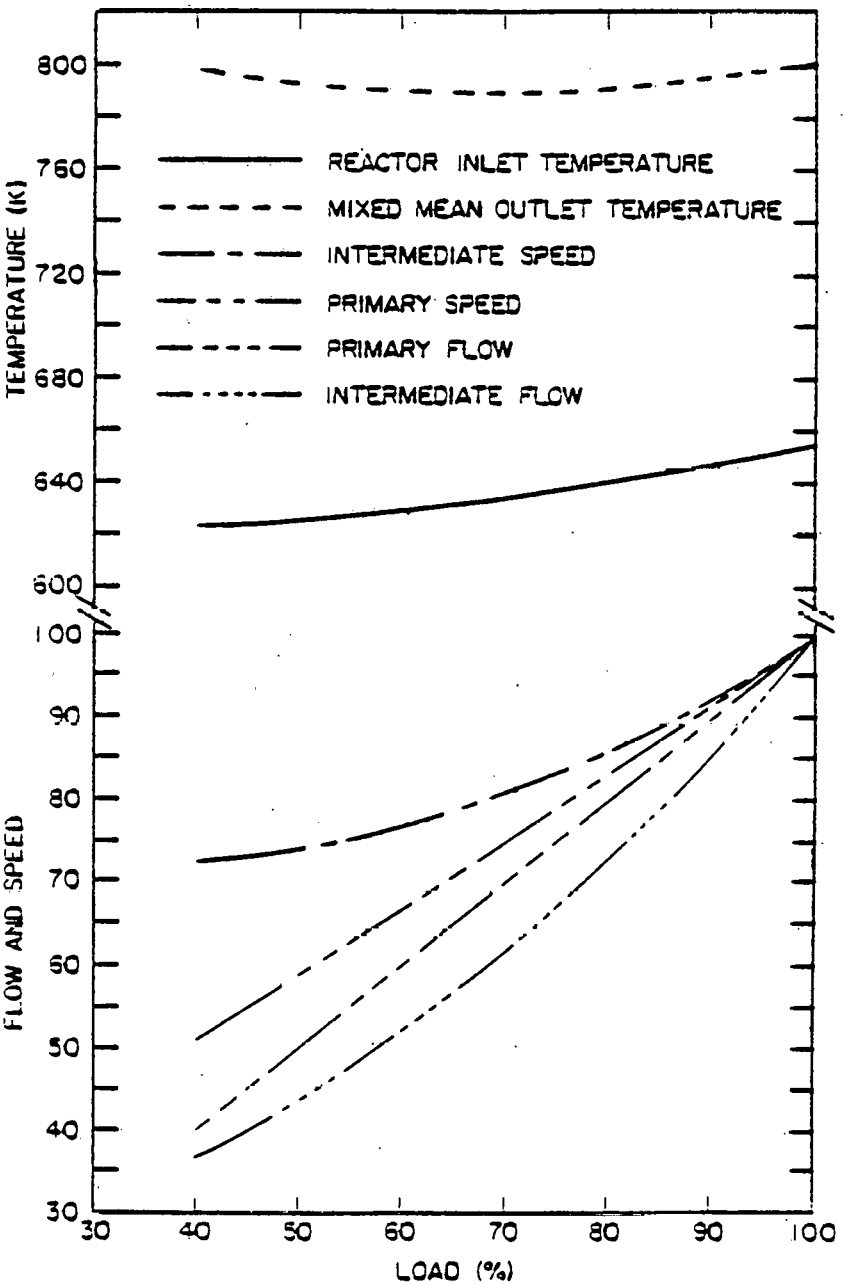

Figure 2. Part Load Profile

Reactor Power Control

The primary control rods are used for both power regulation and reactor shutdown, while the secondary control rods are used for shutdown only. The present model represents the primary control rods by several banks which are assumed to be ganged according to a specified scheme and the reactivity worth of each rod bank is given by first order perturbation theory[8] as:

$$\rho_{PR} = \sum_{i=1}^{M} \rho_{max,i} \left[(Z_i/Z_{max,i}) - \frac{1}{2\pi} \text{Sin } (2\pi Z_i/Z_{max,i}) \right] \tag{5}$$

The control rod position is regulated by the reactor power controller and rod drive mechanism. The reactor control system positions the control rods to reach the desired reactor thermal power, sodium and steam temperatures according to the part load profile. The output of the controller is sent to the power dead zone and saturation circuit limits of the control rod rates. Finally, the signal is divided into an analog magnitude signal and a digital direction signal for use as demands to the control rod drive mechanism actuator.

The input circuitry to each controller accepts on-off inputs for IN, OUT and HOLD commands and provides the required action. The IN command steps a single rod down in the core at a predetermined rate. The OUT command steps a single rod up out of the core at a predetermined rate (not necessarily the same as the IN rate) and the HOLD command maintains the rod in its present position (no motion); that is:

$$\frac{dZ_i}{dt} = \begin{cases} V_{down} & \text{IN Command} \\ V_{up} & \text{OUT Command} \\ 0 & \text{HOLD Command} \end{cases} \tag{6}$$

Sodium Flow Control

The dynamics of sodium flow inside the primary and intermediate systems are governed by the momentum equation which can be written as[4,9]:

$$\left(\frac{\ell}{A}\right) \frac{dW}{dt} + (P_{in} - P_{out}) + \delta P_g + \delta P_f + \delta P_m + \delta P_p = 0 \tag{7}$$

The pump pressure rise, δP_p is dependent on pump speed and sodium flow rate, as described by Madni, et al.[9]

The dynamics of the pump is governed by the torque balance equation for the shaft and rotating assembly[3,4,9] as:

$$\left(\frac{2\pi}{60}\right)\left(\frac{I\Omega_D}{\Gamma_D}\right) \frac{d\alpha}{dt} = \beta_{Mt} - \beta_{F\ell} - \beta_{Fr} \tag{8}$$

The hydraulic torque, β_{Fl}, and the friction torque, β_{Fr} are complicated functions of pump operating conditions and can be found elsewhere.[3,9]

During normal operation, the drive motor torque is adjusted by the controller action, in order to maintain the desired operating conditions. For example, a slight decrease in load causes a reduction in the motor torque which in turn leads to a decrease in pump speed and eventually the sodium flow rate through the variation in pump head, δP_p.

There are various methods for achieving speed control through adjustment of the drive motor torque.[10] They include: (1) changing the number of poles, (2) changing the frequency, (3) changing the external resistance, and (4) varying the hydraulic coupling. The method applied depends on the motor type, and the adequacy of control over the desired operating regime. In the present analysis, we will discuss the frequency and the rheostatic methods for speed control.

The torque of the squirrel cage motor can be written as[10]:

$$\beta_{Mt} = (a_1 \, s + \frac{b_1}{s})^{-1} \tag{9}$$

where a_1, b_1 are constants characterizing the motor behavior and s is the slip ratio defined by $1 - (\Omega_D/\Omega_s)\alpha$, Ω_s being the synchroneous speed (rpm) which is related to frequency f(Hz) and the number of pairs of poles p by (60 f/p).

The torque of the wound rotor induction motor can also be represented by a similar relationship[10]:

$$\beta_{Mt} = (a_2 \frac{s}{R} + b_2 \frac{R}{s})^{-1} \tag{10}$$

and,

$$R = 1 + \frac{R_{ext}}{R_M} \tag{11}$$

where a_2, b_2 are constants characterizing the motor behavior, R is the external resistance parameter, and R_{ext} is the variable external resistance provided by a liquid rheostat actuator and added in series to R_M, the motor rotor resistance (Ω) which is related to the liquid rheostat electrode position y according to the following equation:

$$R_{ext} = R_{max} \, (1 - y)^3 \tag{12}$$

The variable frequency or the liquid rheostat electrode position can be simulated using a second order equation representing a mechanical actuator behaving as a damped harmonic oscillator[6]:

$$\frac{1}{\omega_n^2} \frac{d^2h}{dt^2} + \frac{2\zeta}{\omega_n} \frac{2h}{dt} + (h - h_i) = Tr \tag{13}$$

where ω_n is the natural frequency; ζ is the damping coefficient, h is the actuator output (frequency or the electrode position), h_i is the initial output, and Tr is the trim signal from the last unit controller.

Steam Generator Control

The purpose of steam generator control system is to maintain the temperature, pressure and flow rates at the desired level for both normal and off normal operating conditions. The steam generator control systems consist of (a) feedwater system, and (b) turbine and dump flow mechanism.

The recirculation type steam generator consists of a steam drum, evaporators and superheaters, and a steam header. The feedwater flow rate is controlled in order to maintain a desired steam drum water level and minimize the difference between the feedwater flow into the drum and the saturated steam flow out of the drum. The steam flow rate out of the steam header is controlled based on near constant pressure at the turbine. To enable the nuclear steam supply system to follow turbine load reductions which may exceed large step or ramp changes, an artificial steam load is incorporated. This load is created by dumping steam from the steam header to either condenser and/or atmosphere. The dump system is controlled to give the required ramp load changes to prevent reactor scram. Following the trip, the dump system is switched to a closed loop pressure control mode based on constant header pressure.

The steam generator unit controller is identical to that described earlier. Here, the controller output is used either to adjust the feedwater pump speed and/or to change a valve stem position.

The valve dynamics is represented by a first order system accounting for deadband and hysterisis effects. That is:

$$\frac{dS_v}{dt} = \begin{cases} \dfrac{1}{\tau_{vo}} & Tr \geq Tr_{max} \quad \text{(opening)} \\ 0 & Tr_{min} < Tr < Tr_{max} \quad \text{(no motion)} \\ \dfrac{1}{\tau_{vc}} & Tr \leq Tr_{min} \quad \text{(closing)} \end{cases} \tag{14}$$

and the fractional stem position S_v is bounded; i.e., $S_{min} \leq S_v \leq S_{max}$. Here, S_{min} is the minimum stem position, S_{max} is the maximum stem position, τ_{vo} is the time to open from S_{min} to S_{max}, and τ_{vc} is the time to close from S_{max} to S_{min}. The deadband and hysterisis effects prevent the valve from opening if the trim signal is smaller than a maximum limit, Tr_{max}, and from closing if the trim is greater than a minimum limit Tr_{min}.

Non-Linearity Effects

The control systems discussed in this paper have been incorporated into the SSC code. SSC models and numerically solves the conservation equations described in the previous subsections, in their truly nonlinear forms.

Many of the existing control system design and analysis studies use linearized approximations representative of the nonlinear systems in the vicinity of the steady-state operating conditions. While much useful information can be obtained from such studies, it frequently is desirable or necessary to consider nonlinearities in control system design and operation.

In order to demonstrate the comparison between the linear and nonlinear models, a linearized version of the flow-speed control was developed by using Taylor series expansions of the nonlinear terms in the coolant momentum and the pump angular momentum equations around the steady-state 100% operating conditions. The two models were compared for a transient resulting from a 20% step reduction in load demand. Figure 3 shows the system response for both linear and nonlinear models using identical controller settings (gains, time constants, etc.).

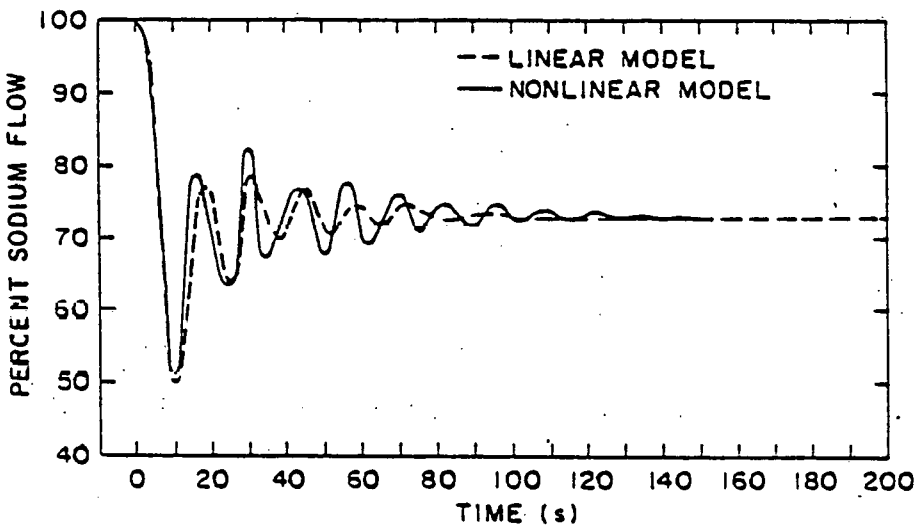

Figure 3. Comparison of Linear and Non-Linear Models.

It is evident that the flow oscillations are less severe and tend to damp-out much sooner for the linear model than for the nonlinear model. Several perturbations were tested and it was found that the agreement between the linear and nonlinear models improve as the input perturbations get less severe. It was also observed that for a just stable control system setting with the linearized model, the nonlinear model was unstable.

RESULTS AND DISCUSSIONS

The present model has been tested using the Clinch River Breeder Reactor Plant (CRBRP) reference design data where available.[11]

Table I summarizes various feedback elements and their associated control settings for reactor power, primary and intermediate flow-speed control systems. Table II sets forth the primary control rod banking data.

TABLE I
Plant Control System Data

Unit Controller			τ_m(s)	K	R(s^{-1})	τ_D(s)	ε_o	Actuator Constants
Reactor Power Controller		Steam Temperature	0.20	2.0	0	0	0	$v_{up} = 3.81 \times 10^{-3}$ m/s $v_{down} = -3.81 \times 10^{-3}$ m/s
		Core Mixed Mean Temp.	0.20	2.0	0	0	0	
		Neutron Flux	0.05	1.0	0	0	0.005	
Flow Controller	Primary	Reactor Inlet Temp.	0.20	1.0	0	0	0	$a_1 = 0.577$ $b_1 = 0.065$ $\zeta = 1.0$ (critically damped) $\omega_n = 0.375$ (s^{-1}) $\Omega_D = 1116$ rpm
		Sodium Flow	0.50	1.0	0	0	0	
		Pump Speed	0.02	1.0	0.10	0	0.005	
	Intermediate	Steam Pressure	0.15	1.0	0.02	0	0	$a_1 = 0.577$ $b_1 = 0.065$ $\zeta = 1.0$ $\omega_n = 0.375$ $\Omega_D = 1116$ rpm
		Sodium Flow	0.50	1.0	0.20	0	0	
		Pump Speed	0.02	1.0	0.10	0	0.005	

TABLE II
Primary Control Rod Banking Data[11]

Location	$\rho_{max,i}$(\$)	$Z_{max,i}$(m)	ρ_i(\$)	Z_i(m)
6-R7F	12.17	0.940	3.49	0.300
6-R7C	11.00	0.940	6.72	0.584
2-R4	2.95	0.940	2.95	0.940

Three representative anticipated transients without scram were simulated, they are: (1) a 10 cent step insertion of reactivity, (2) a 25 cent step insertion of reactivity and (3) a 10% ramp change in load demand in 40 seconds.

Figure 4 shows the reactor system response to a 10 cent and a 25 cent step insertions of reactivity at time zero of the transient. The total reactivity is seen to jump from 0 to 0.10 and 0.25 dollar at time zero causing a sharp rise in the neutron flux (power level) and, hence, an increase in reactor temperatures. The controller tries to correct for the disturbance by driving the regulatory bank into the core, until finally the neutron flux and the core mixed mean sodium temperature reach their respective setpoints as calculated by the plant supervisory controllers.

It is important to note that all of the automatic shutdown functions of the Plant Protection System (PPS), which would normally override the controllers in an event that the PPS settings are exceeded (e.g., 115% overpower signal) were inactivated.

Figure 5 illustrates the plant response to a typical plant unloading of 10% in 40 seconds. It is seen that as the load demand is reduced, the plant control system responds by driving the regulating rod into the reactor as well as reducing the drive motor torque on both primary and intermediate pumps causing the desired reduction in the feedback variables to within the accuracies of their deadband settings.

From the results presented, the following conclusions are derived: (1) the representation of plant control systems in a large system simulation code is an essential tool for the study of ATWS event in LMFBR systems, and (2) the nonlinearity of the plant over a wide range of operating conditions necessitates a nonlinear simulation of the overall system.

For future work, it is essential to include improved models to simulate the motor-generator set and its influence on the sodium flow-speed control system. The influence of unit controller settings and feedback cascading on the predicted response of the plant requires further investigation. The interaction of the plant protection and control systems needs to be studied to determine the possibility of PCS adversely affecting or preventing the PPS actions.

ACKNOWLEDGEMENT

The authors acknowledge the invaluable help of J. G. Guppy and R. J. Kennett in interfacing the present model into the SSC code. Thanks are also due to I. K. Madni for reviewing the paper, and to Ms. D. Clay for her skillful typing of this manuscript.

This work was performed under the auspices of the United States Nuclear Regulatory Commission.

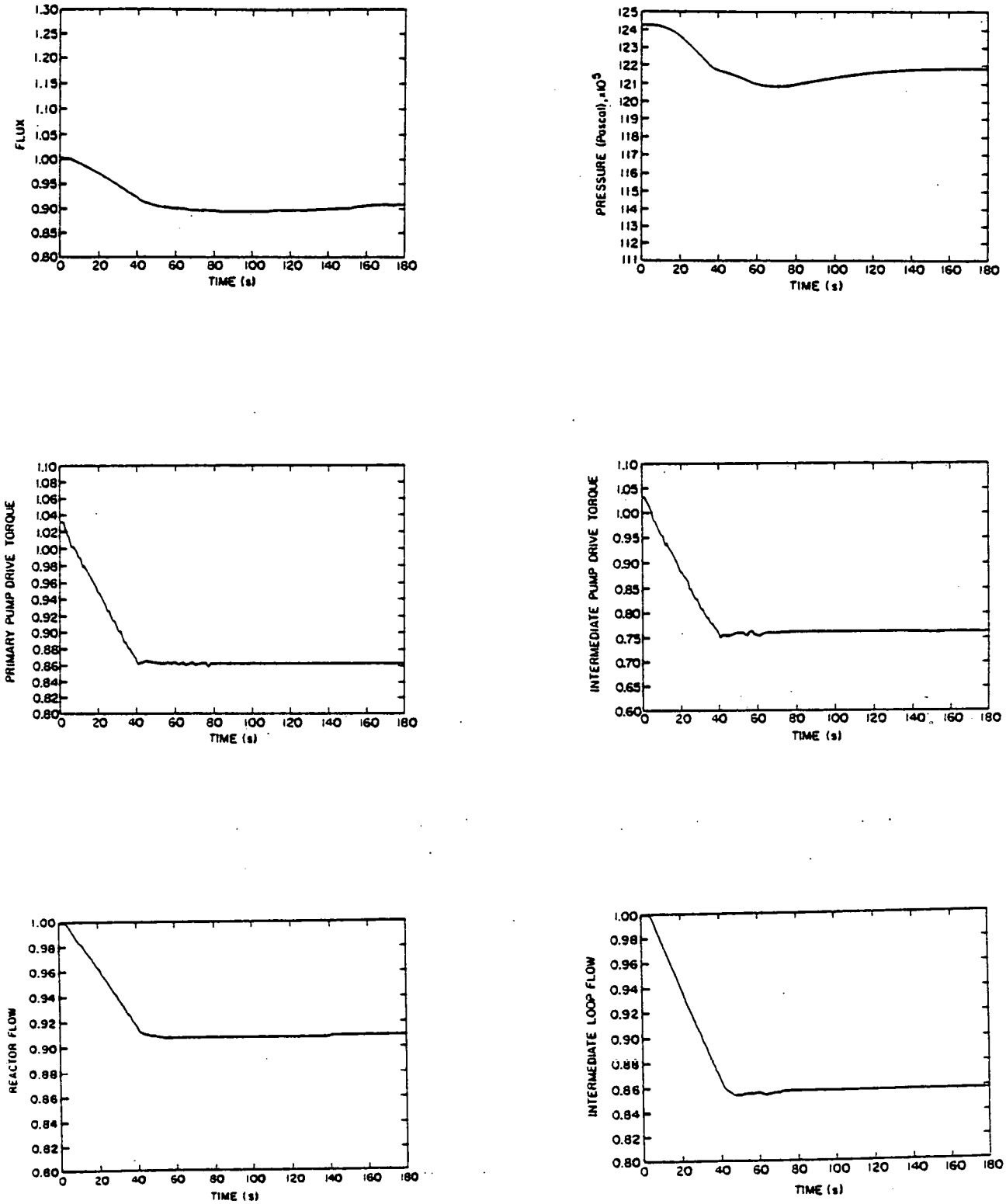

Figure 5. System Response to a Transient Resulting from a 10% Ramp Change in Power Demand in 40 Seconds.

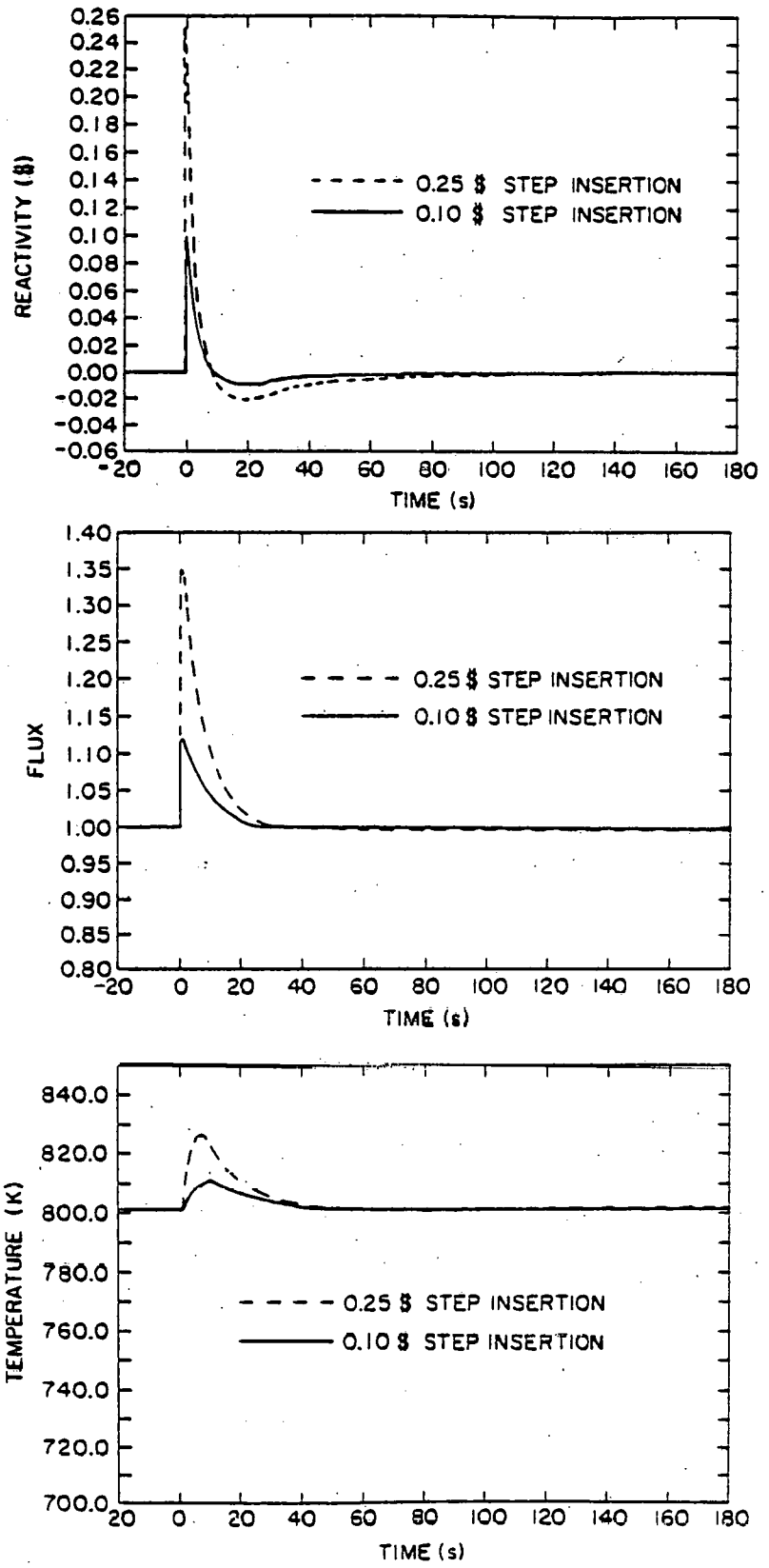

Figure 4. System Response to 10 cent and 25 cent Step Insertion of Reactivity Transient.

NOMENCLATURE

A	Area (m^2)
a	Motor constant
b	Motor constant
c	Polynomial coefficient
f	Frequency (Hz)
h	Actuator output
I	Inertia ($kg-m^2$)
K	Gain
L	Load
ℓ	Length (m)
P	Pressure (N/m^2)
p	Pairs of poles
R	Repeat rate, resistance (s^{-1}, Ω)
S	Stem position
s	Slip
Tr	Trim
V	Control rod speed (m/s)
W	Flow rate (kg/s)
X	Process variable
y	Electrode position
Z	Rod position (m)
α	Relative speed
β	Relative torque
ε	Error
ζ	Damping coefficient
τ	Time constant (s)
Ω	Speed (rpm)
ω	Natural frequency (s^{-1})
Γ	Torque (N-m)

Subscripts:

D	Demand/derivative/design
ext	External
f	Friction
Fl	Fluid
Fr	Friction
g	Gravity
M	Measured, momentum
Mt	Motor
s	Synchronous
SP	Set point

REFERENCES

1. "LMFBR Demonstration Simulation Model, DEMO," Westinghouse Advanced Reactors Division, WARD-D-0005 (Rev. 4), (1976).

2. D. L. HETRICK and G. W. SOWERS, "BRENDA: A Dynamic Simulator for a Sodium-Cooled Fast Reactor Power Plant," U. S. Nuclear Regulatory Commission, NUREG/CR-0244 (1978).

3. K. B. CADY et al., "EPRI-CURL: Dynamic Analysis of Loop-Type LMFBRs," Electric Power Research Institute, EPRI-NP-1001 (1979).

4. A. K. AGRAWAL et al., "An Advanced Thermohydraulic Simulation Code for Transients in LMFBRs (SSC-L)," Brookhaven National Laboratory, BNL-NUREG-50773 (1978).

5. D. M. CONSIDINE, (editor), *Process Instruments and Controls Handbook*, Gordon and Breach, Science Publishers, Inc., New York (1969).

6. D. R. COUGHANOWR and L. B. KOPPEL, *Process Systems Analysis and Control*, McGraw-Hill Book Co., New York (1965).

7. "Operator's Manual for Vutronik Cascade Control Stations," Operator's Manual 37-01-05, Issue 2, Honeywell Industrial Division, Fort Washington, Pennsylvania (1973).

8. J. R. LAMARSH, *Introduction to Nuclear Reactor Theory*, Addison-Wesley Publishing Company, Inc., Massachusetts (1961).

9. I. K. MADNI, E. G. CAZZOLI, and A. K. AGRAWAL, "A Single-Phase Sodium Pump Model for LMFBR Thermal-Hydraulic Analysis," in *Proc. of International Meeting on Fast Reactor Safety Technology*, August 19-23, 1979, Seattle, Washington.

10. P. L. ALGER, *Induction Machines*, Gordon and Breach Science Publishers, New York (1970).

11. Clinch River Breeder Reactor Plant Preliminary Safety Analysis Report, Project Management Corporation (1975).